Direct torque control of electric vehicle drives using hybrid techniques

Hallikeri Basappa Marulasiddappa, Viswanathan Pushparajesh
Department of Electrical and Electronics Engineering, JAIN (Deemed to be University), Bangalore, India

ABSTRACT

Permanent magnet synchronous motors (PMSM) have the capability of delivering a high torque-to-current ratio, better efficiency and low noise. Because of the above-mentioned factors, PMSMs are commonly employed in variable speed drives, especially in electric vehicle (EV) applications. Without the usage of electromechanical devices, the conventional direct torque control (DTC) can control the speed and torque of PMSM. DTC is highly efficient, fast-tracking and provides smooth torque while limiting its ripple during transient periods. There are many benefits to using a DTC-controlled PMSM drive, including quick and reliable torque reaction, high-performance control speed, and enhanced performance. This research examines the use of the DTC approach to enhance the speed and torque behavior of PMSM. The jellyfish search optimizer (JSO) is used to adjust the DTC's responsiveness and tailor the controller's best gains. In order to train the adaptive neuro-fuzzy inference system (ANFIS) controller, JSO data are utilized. The simulation outcomes demonstrate that the proposed JSO-ANFIS controller achieves a minimal torque ripple of 0.26 Nm and preserves the speed with a harmonic error of 1.21% while contrasted to existing methods.

Corresponding Author:

Viswanathan Pushparajesh
Department of Electrical and Electronics Engineering, JAIN (Deemed to be University)
Bangalore-Kanakapura Main Road, Ramanagara District-562 112, India
Email: pushparajesh.v@gmail.com

NOMENCLATURE

$\overrightarrow{trend}$	: Ocean current	C_o	: Constant
n_{pop}	: Number of jellyfish	ω_{max}	: Speed at maximum rate
X^*	: Best position	α	: Momentum constant
η	: Learning rate	X_0	: Initial population
$X_i(t+1)$	: New position	$X_{i,d}$	: Position of ith jellyfish in d^{th} dimension
β	: Distribution coefficient	a_{ij}, b_{ij}, c_{ij}	: Input membership function
$rand(0,1)$	: Random variables	ω_{ref}	: Reference speed
U_b	: Upper bound	ω_{act_i}	: Actual speed
L_b	: Lower bound	t	: Current iteration
γ	: Motion coefficient	n	: Step time
f	: Function of position		

LIST OF ABBREVIATIONS

PMSM : Permanent magnet synchronous motors

DTC	: Direct torque control
JSO	: Jellyfish search optimizer
ANFIS	: Adaptive neuro-fuzzy inference system
SVPWM-DTC	: Space vector pulse width modulation-based DTC
DCF-MPDSC	: Dual cost function model predictive direct speed control
EV	: Electric vehicle
TSMPC	: Tolerance sequential model predictive control
FST	: Flexible switching table
ZST	: Zero sequence torque
IL-DTC	: Improved iterative learning direct torque control
MPDTC	: Model predictive direct torque control
FOC	: Field-oriented control

1. INTRODUCTION

In past decades, PMSMs were identified as promising materials for EV applications because of their low weight, high reliability, speed control variation, low distortion, and efficient performance [1]. In the context of EV traction, a quick and reliable torque response of the electrical drive is necessary to satisfy the instantaneous torque demand ordered by the operator via drive movement [2]. Additionally, the PMSM drive should be capable of recovering quickly from system disruptions in terms of torque and speed. These are a few of the demands on the EV's performance that must be met to match the driving characteristics [3]. In order to torque ripple minimization with enhancing the steady-state performance, FOC is utilized. FOC enhances the efficacy of the dynamic response [4], [5]. However, when the temperature varies, this technique becomes susceptible to even minor changes in the parameter.

To enhance the performance of the PMSM motor, numerous control strategies are suggested. The shortcomings of FOC were replaced by a brand-new method known as DTC by Bao *et al.* [6]. Torque and flux can be immediately controlled by DTC by making the PMSM drive more effective. By using the torque error and motor speed to determine the active vector, complicated mathematical processes are avoided [7]. But it also makes the monitoring system noisy [8]. To provide appropriate steady-state performance, torque, stator flux disturbances and high-frequency components have to be eliminated [9]. The existing solutions completely disregard rotating components and solely use active vectors, or a combination of dynamic matrices and zero matrices [10].

To solve the synchronous torque and flux in the PMSM machine, Pushparajesh *et al.* [11] developed TSMPC based on lexicographic technique. However, the assumptions made in this study are that a best voltage vector as well as every cost function's limitation was confined to a mere lower limit. For the DTC of PMSM, Nasr *et al.* [12] suggested a FST. ZST generally does not permit the reversal of revolution, which is its fundamental error. By increasing the area with a duty cycle angle to improve the torque and speed response, Zhang *et al.* [13] showed a methodology that was known as: MPDTC. A model-free deep reinforcement learning torque regulator was developed by Schenke and Wallscheid [14]. Yet, the reinforcement learning was not applied to dynamic stability theory. To significantly minimize the torque fluctuations for PMSM drive, Mohammed *et al.* [15] demonstrated an IL-DTC. Unfortunately, parameter variations restricted the usage of SPMSM which reduced the motor's ability to manage torque disturbances. In PMSM, to enhance the efficiency, a combined mechanism [16] was developed. But leakage current was the root of the problem. For PMSM, SVPWM-DTC [17] was proposed; however, because of the bandwidth restriction, the motor experienced significant torque ripple. For PMSM drives, a brand-new DCF-MPDSC [18] with duty ratio minimization was introduced. Every DTC computation currently in use is carried out in a stationary reference frame without the qualitative data of the rotor location [19]. Because of its simplicity, it can run each computing cycle quickly and with a high sample frequency [20]. The ripple will roughly decrease for every increase in the sampling frequency [21]. The excessive torque ripple of the DTC control was a significant drawback. This generally does not pose a problem in some applications since the ripple is filtered by the rotor and the load inertia, but in other applications like electric vehicles, low torque ripple is crucial [22].

In this research, an approach based on JSO-ANFIS is used to present the solution to the aforementioned problem. The main contribution of current study is stated as: i) the JSO-ANFIS-based DTC of the PMSM drive is adopted to eliminate torque ripples and improve the speed; ii) a variable switching table for the DTC of the PMSM is computed to enhance steady state and dynamic functionality; and iii) in stationary reference, the PMSM's dynamic behavior is described to prevent complex frame transportation.

The organization of current research is specified; the proposed method with the statistical equations are explained in section 2. The simulation outcomes as well as the comparison evaluation with conventional approaches are represented in section 3. At last, the research conclusion is briefly and clearly explained in section 4.

2. METHOD

Here, the speed and torque of the PMSM drive depend on JSO-ANFIS-based DTC control. JSO is used to optimize the ANFIS learning variable in a variety of functioning scenarios. Creating a DTC system to enhance the PMSM drive's effectiveness is considered as the major goal of the current research which enables smooth torque output as well as better speed control monitoring.

2.1. DTC of PMSM

In the traditional DTC scheme, the regulation of a PMSM motor in an EV obtains various fluctuations, those of which are surpassed by employing the proposed DTC control. Figure 1 illustrates the overall block diagram for the suggested technique. During the operation of classical DTC, the steady state signals show clear flux linkage vectors within the six sectors boundary [23]. Enhancing the effectiveness of the PMSM by focusing on continuous torque response and speed by using hybrid JSO-ANFIS-based DTC control is considered as the main objective in this work. Table 1 represents the switching table of DTC for PMSM drive, wherein ON and OFF states are denoted by codes 1 & 0 correspondingly.
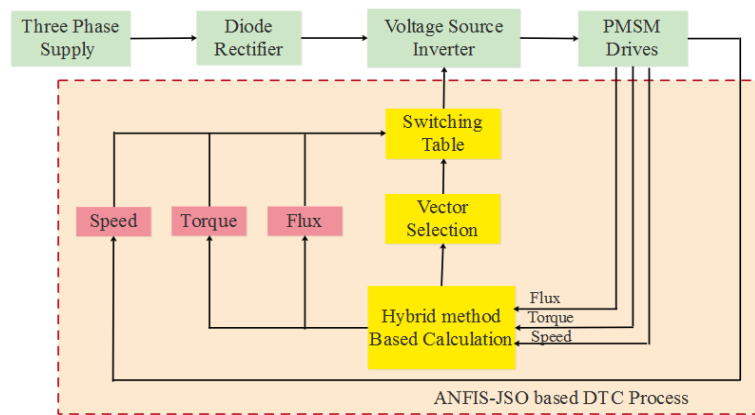

Figure 1. Block diagram of the proposed approach

Table 1. Switching table of DTC

Flux	Torque	Sector					
		1	2	3	4	5	6
1	1	V2	V3	V4	V5	V6	V1
	0	V0	V7	V0	V7	V0	V7
	-1	V6	V1	V2	V3	V4	V5
0	1	V3	V4	V5	V6	V1	V2
	0	V7	V0	V7	V0	V7	V0
	-1	V5	V6	V1	V2	V3	V4

2.2. Jellyfish search optimizer

Globally, jellyfish are mostly available in greater depths under the sea [24]. By combining all the paths in the sea used by the jellyfish, the ocean current's main trend is found which is represented in (1).

$$\overrightarrow{trend} = \frac{1}{n_{pop}} \sum \overrightarrow{trend_\iota} = \frac{1}{n_{pop}} \sum (X^* - e_c X_i) = X^* - e_c \frac{\sum X_i}{n_{pop}} = X^* - e_c \mu \tag{1}$$

Then fix $df = e_c \mu$ (2)

Consequently, (3) represents the updated ($\overrightarrow{trend}$),

$$\overrightarrow{trend} = X^* \tag{3}$$

n_{pop} is number of jellyfish, e_c is attraction control variable, X^* is best position of jellyfish. Every jellyfish's mean position, and the distance between a current best location of jellyfish as well as the average location is df which is given in (4).

$$df = \beta \times \sigma \times rand^f(0,1) \tag{4}$$

$$\text{Fix } \sigma = rand^\alpha(0,1) \times \mu \tag{5}$$

$$\text{Later, } df = \beta \times rand^f(0,1) \times rand^\alpha(0,1) \times \mu \tag{6}$$

For further updates, (6) is modified as (7) and (8).

$$df = \beta \times rand(0,1) \times \mu \tag{7}$$

$$e_c = \beta \times rand(0,1) \tag{8}$$

Therefore,

$$\overrightarrow{trend} = X^* - \beta \times rand(0,1) \times \mu \tag{9}$$

using (10), all the jellyfish new location is determined.

$$X_i(t+1) = X_i(t) + rand(0,1) \times \overrightarrow{trend} \tag{10}$$

Then, (10) is modified and as (11),

$$X_i(t+1) = X_i(t) + rand(0,1) \times \overrightarrow{trend} \times X^* - \beta \times rand(0,1) \times \mu \tag{11}$$

where, $\beta > 0$ is the distribution coefficient, [$\beta = 3$].

In both passive (type A) as well as active (type B) ways, Jellyfish can swim with their groups. Type A is simply known as motion of jellyfish within their locations, and (12) represents all jellyfish's new location (12),

$$X_i(t+1) = X_i(t) + \gamma \times rand(0,1) \times (U_b - L_b) \tag{12}$$

U_b is Upper bound, L_b is Lower bound, $\gamma > 0$ is coefficient of movement, whereas, $\gamma = 0.1$ is obtained using (12). Moreover, (13) expresses this effort which is deliberated as a local exploration's operative manipulation,

$$\overrightarrow{Step} = X_i(t+1) - X_i(t) \tag{13}$$

$$\text{Here, } \overrightarrow{Step} = rand(0,1) \times \overrightarrow{Direction} \tag{14}$$

$$\overrightarrow{Direction} = \begin{cases} X_j(t) - X_i(t) \text{ if } f(X_i) \geq f(X_j) \\ X_i(t) - X_j(t) \text{ if } f(X_i) < f(X_j) \end{cases} \tag{15}$$

here, f is location X's function.

$$\text{Thus, } X_i(t+1) = X_i(t) + \overrightarrow{Step} \tag{16}$$

The movement type over a period of time is defined by utilizing a temporal control mechanism. The time control system comprises of a time control function $c(t)$ and constant C_o which are used to control the ability of jellyfish. The time control randomly changes between 0 &1, thus the C_o's accuracte value remains unknown. So, C_o is fixed to 0.5, which is expressed in (17).

$$C(t) = \left| \left(1 - \frac{t}{Max_{iter}}\right) \times (2 \times rand(0,1) - 1) \right| \tag{17}$$

Thus, the (18) represents the written map,

$$X_{i+1} = \eta X_i(1 - X_i), 0 \leq X_0 \leq 1 \tag{18}$$

here, X_i is i^{th} jellyfish location's chaotic value, X_0 is initial population in [0,1], where $\eta = 4.0$.

Due to spherical shape of earth, a jellyfish can get back to the contrary bound when it gets out from the search area which is given in (19),

$$\begin{cases} X'_{i,d} = (X_{i,d} - U_{b,a}) + L_b(d) \ if \ X_{i,d} > U_{b,d} \\ X_{i,d} = (X_{i,d} - L_{b,d}) + U_b(d) \ if \ X_{i,d} < L_{b,d} \end{cases} \tag{19}$$

$X_{i,d}$ is i^{th} jellyfish's location in d^{th} dimension, and $X'_{i,d}$ is updated position.

2.3. ANFIS

This control technique actually combines the processes of fuzzy as well as ANN [25]. ANFIS is used to create the torque standard from speed error variations, each time. The network comprises 20 nodes and undergoes 12 epochs of training. Two-Gaussian membership functions are analyzed by each node in this layer, after which, the input parameters are transferred to the following layer. The non-linear element is included in each iterative count which is described as input MF a_{ij}, b_{ij}, c_{ij} which is modified via the (20).

$$a_{ij}^{(1)}(n + 1) = \alpha \left(a_{ij}^{(1)}(n) \right) + \eta \left(-\frac{\partial E(n)}{\partial a_{ij}^{(1)}} \right)$$

$$b_{ij}^{(1)}(n + 1) = \alpha \left(b_{ij}^{(1)}(n) \right) + \eta \left(-\frac{\partial E(n)}{\partial b_{ij}^{(1)}} \right)$$

$$c_{ij}^{(1)}(n + 1) = \alpha \left(c_{ij}^{(1)}(n) \right) + \eta \left(-\frac{\partial E(n)}{\partial c_{ij}^{(1)}} \right) \tag{20}$$

Step time is stated as n; learning rate is stated as η; steepest momentum constant is referred to as α.

2.4. JSO-optimized ANFIS

In this section, under different PMSM drive operating conditions JSO-optimized learning parameters for ANFIS are described. To minimize the next objective function denoted by (21), the algorithm constraints are chosen. After that, the selected constraints are intended as the fitness function for optimization to ensure consistency and achieve higher restraint in the event of unanticipated load disruption and speed differences.

$$J_1(S) = H_1 + H_2 \tag{21}$$

$$H_1 = \sqrt{\frac{\sum_m^{i=1}(\omega_{ref} - \omega_{act_i})^2}{m}}$$

$$H_2 = \begin{cases} \omega_{max} - \omega_{ref} & if \ \omega_{max} > \omega_{ref} \\ 0 & Otherwise \end{cases}$$

ω_{max} is stated as the speed at maximum level; ω_{act_i} and ω_{ref} is referred to as an actual and reference speed; m is stated as Sample count; the range of tuning variables are declared in (22) and (23).

$$0 \leq \eta \leq 2 \tag{22}$$

$$0 \leq \alpha \leq 2 \tag{23}$$

3. SIMULATION RESULTS AND DISCUSSION

Numerous features of direct torque control for PMSM drives are discussed in this study. The JSO-ANFIS is implemented and simulated using following setup: This research is implemented in MATLAB R2020a tool using the Intel Core i3 processor, Windows 8 OS and a RAM of 8 GB. Moreover, Table 2 shows the ratings of the simulation model. The creation of DTC regulation in the PMSM motor utilizing JSO-ANFIS, is experimentally executed by using MATLAB is demonstrated in Figure 2. Table 2 contains all of the control variables for the simulation environment. A 10-second sample rate is specified. Specifically, the inertia bands are set to 1.8 Nm and 0.088 Wb.

Figure 3 display the speed performance of ANFIS. The motor's speed is being used as a response, and the difference between it and to determine the speed inconsistency, the reference speed is used. A reference value of 4,000 along with the projected speed error, variation, and error, are all sent to the JSO-ANFIS controller. Similarly, Figure 4 display the ANFIS torque.

Table 2. Rating of the simulation model

| Parameters	Values
Moment of inertia	0.0017 kgm^2
Rated speed	4000 rpm
Stator resistance	0.636 ohm
Viscous friction	0.0017 kgm/s^2
Weighting factor	1
Rated current	11.36 A
Flux	0.088 Wb
q-axis inductance	0.02 H
Rated torque	1.8 Nm
Number of pole pairs	2
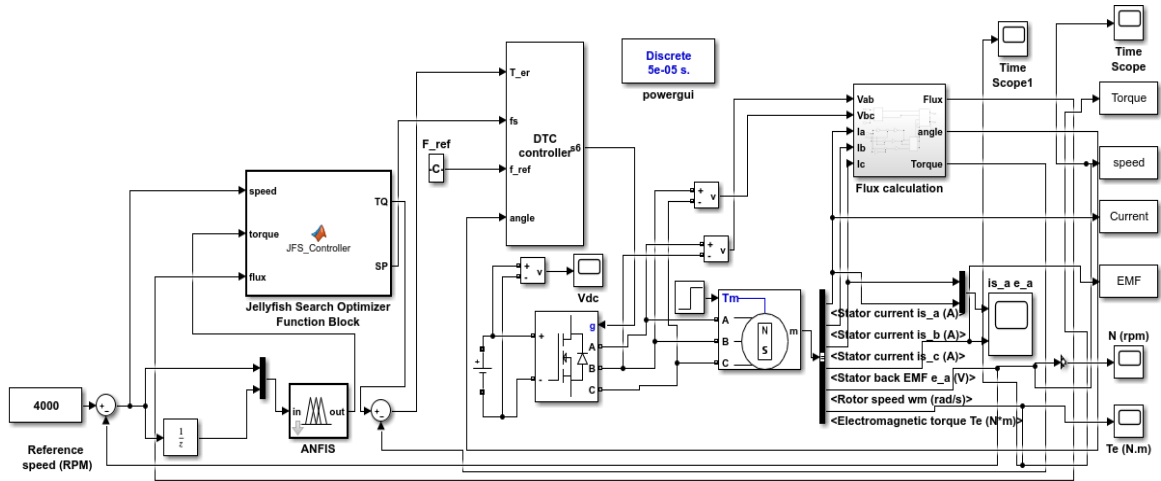
Figure. 2 Simulation model of PMSM with JSO-ANFIS
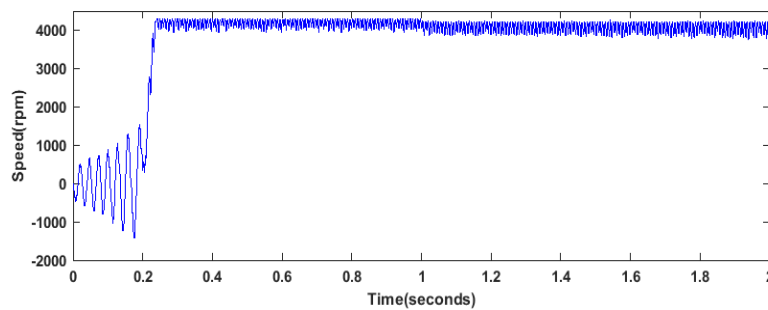
Figure 3. Speed performance of ANFIS
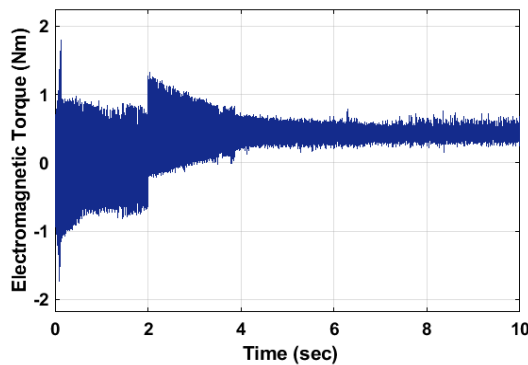
Figure 4. Torque performance of ANFIS

The simulation findings demonstrate that JSO-ANFIS achieves superior performance related to the ANFIS. Additionally, it might make the system more stable. The suggested JSO-ANFIS outperformed conventional systems by achieving a stable state in 1.7 seconds. The suggested JSO-optimized ANFIS, conventional proportional integral derivative (PID), and ANFIS are used to evaluate the steady-state assessment and other constraints (settling time, rising time, and overshoot time) which are tabulated in Table 3. Figures 5 to 7 show the JSO-ANFIS controller's findings for speed and torque. The comparison of transient response with conventional controllers is shown in Table 4. Even while traditional PID and ANFIS operate superior in terms of rise and settling times, overshoot is more obvious and invalidates all other transient quality objectives.

Table 3. Comparison for transient response

| Constraints	PID	ANFIS	GEO-ANFIS	JSO-ANFIS
Rising time (sec)	0.105	0.053	0.034	0.029
Overshoot time (%)	7.888	6.043	5.592	5.577
Settling Time (sec)	0.341	0.19	0.12	0.10
Steady State (sec)	3.5	2.1	1.9	1.7
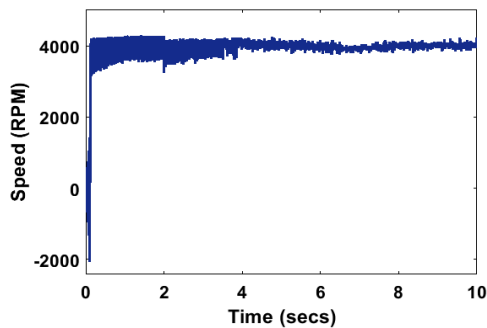
Figure 5. Speed performance of JSO-ANFIS
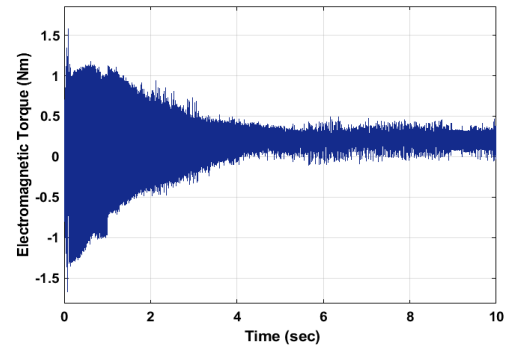


Figure 6. Torque performance of JSO-ANFIS
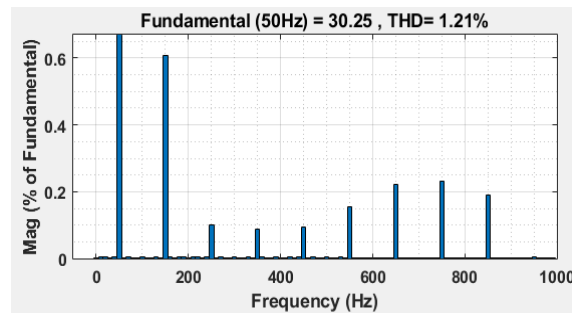
Figure 7. Harmonic analysis

The evaluation of torque ripple is shown in Table 4 which evidently proves that compared to current SVPWM-DTC [16] and ANFIS, the suggested JSO-ANFIS achieves a smaller torque ripple. Also, when related with previous models of SVPWM-DTC [16], ANFIS, and GEO-ANFIS, which reached 0.6 Nm, 0.53 Nm, and 0.44 Nm correspondingly, the suggested JSO-ANFIS obtains a smaller torque ripple of 0.26 Nm. The harmonic evaluation of the PMSM motor is shown in Figure 7. The proposed JSO-ANFIS controller exceeds the currently used DCF-MPDSC [17] and ANFIS controller in the control method.

Table 5 indicates that the proposed JSO-optimized ANFIS obtains 1.21% of greater THD which is better than conventional DCF-MPDSC [17] which attained 4.43%. While replacing the speed regulator using traditional PID as well as JSO-ANFIS controller, the PMSM motor's DTC control with its effective characteristics was enhanced. The suggested JSO-ANFIS controller minimizes the time delay compared to the traditional SVPWM-DTC & DCF-MPDSC controllers, which takes a long time to stabilize.

Table 4. Comparison of torque ripple

Parameters	SVPWM-DTC [16]	ANFIS	GEO-ANFIS	JSO-ANFIS
Torque Ripple (Nm)	0.6	0.53	0.44	0.26

Table 5. THD comparison

Approaches	Values (%)
DCF-MPDSC [17]	4.43
ANFIS	2.33
GEO-ANFIS	2.12
JSO-ANFIS	1.21

4. CONCLUSION

For the past few years, real-time control and DTC control of PMSM drives have achieved a lot of attention as it improves the effectiveness of the system. The outcome of the conventional direct torque control is a large torque as well as flux linkage ripple centered on the 60 degrees sector that included the position signal to choose the appropriate space voltage vector. Here, JSO is used in many situations to maximize the ANFIS learning variables. To achieve closed-loop operation, a speed controller called the JSO-ANFIS is used. The MATLAB/Simulink results demonstrate that the suggested JSO-ANFIS can eliminate the uncertainty problems brought on by speed/load variations. In comparison to the DCF-MPDSC controller, the simulation observed that the proposed technique delivers minimal torque ripple (0.26 Nm) and less THD (1.21%) which enhances system efficiency. The strong formula and rule modules make it easy to design and install the JSO-ANFIS controller. This research project may be expanded in the future using further meta-heuristic approaches or hybrid intelligence methods.

REFERENCES

[1]   F. Ben Salem, "Stator winding fault diagnosis of permanent magnet synchronous motor-based DTC-SVM dedicated to electric vehicle applications," in *Autonomous Vehicle and Smart Traffic*, IntechOpen, 2020, doi: 10.5772/intechopen.88784.

[2]   H. B. Marulasiddappa and V. Pushparajesh, "Review on different control techniques for induction motor drive in electric vehicle," *IOP Conference Series: Materials Science and Engineering*, vol. 1055, no. 1, Feb. 2021, doi: 10.1088/1757-899X/1055/1/012142.

[3]   U. R. Muduli, A. R. Beig, K. Al Jaafari, J. Y. Alsawalhi, and R. K. Behera, "Interrupt-free operation of dual-motor four-wheel drive electric vehicle under inverter failure," *IEEE Transactions on Transportation Electrification*, vol. 7, no. 1, pp. 329–338, Mar. 2021, doi: 10.1109/TTE.2020.2997354.

[4]   D. R. G. Shriwastava, D. N. B. Wagh, and D. S. K. Shinde, "Implementation of DTC-controlled PMSM driven by a matrix converter," *International Journal of Recent Technology and Engineering (IJRTE)*, vol. 8, no. 5, pp. 4420–4424, Jan. 2020, doi: 10.35940/ijrte.E6641.018520.

[5]   M. Wang, D. Sun, W. Ke, and H. Nian, "A universal lookup table-based direct torque control for OW-PMSM drives," *IEEE Transactions on Power Electronics*, vol. 36, no. 6, pp. 6188–6191, Jun. 2021, doi: 10.1109/TPEL.2020.3037202.

[6]   G. Bao, W. Qi, and T. He, "Direct torque control of PMSM with modified finite set model predictive control," *Energies*, vol. 13, no. 1, Jan. 2020, doi: 10.3390/en13010234.

[7]   W. Deng and S. Li, "Direct torque control of matrix converter-fed PMSM drives using multidimensional switching table for common-mode voltage minimization," *IEEE Transactions on Power Electronics*, vol. 36, no. 1, pp. 683–690, Jan. 2021, doi: 10.1109/TPEL.2020.2998686.

[8]   Y. Wang, Y. Zhu, X. Zhang, B. Tian, K. Wang, and J. Liang, "Antidisturbance sliding mode-based deadbeat direct torque control for PMSM speed regulation system," *IEEE Transactions on Transportation Electrification*, vol. 7, no. 4, pp. 2705–2714, Dec. 2021, doi: 10.1109/TTE.2021.3083074.

[9]   X. Wang, Z. Wang, Z. Xu, M. Cheng, and Y. Hu, "Optimization of torque tracking performance for direct-torque-controlled PMSM drives with composite torque regulator," *IEEE Transactions on Industrial Electronics*, vol. 67, no. 12, pp. 10095–10108, Dec. 2020, doi: 10.1109/TIE.2019.2962451.

[10]   W. Deng, H. Li, and J. Rong, "A novel direct torque control of matrix converter-fed PMSM drives using dynamic sector boundary for common-mode voltage minimization," *IEEE Transactions on Industrial Electronics*, vol. 68, no. 1, pp. 70–80, Jan. 2021, doi: 10.1109/TIE.2019.2962408.

[11]   V. Pushparajesh, B. M. Nandish, and H. B. Marulasiddappa, "Torque ripple minimization in switched reluctance motor using ANFIS Controller," *WSEAS Transactions on Systems and Control*, vol. 16, pp. 171–182, Mar. 2021, doi: 10.37394/23203.2021.16.14.

[12]   A. Nasr, C. Gu, S. Bozhko, and C. Gerada, "Performance enhancement of direct torque-controlled permanent magnet synchronous motor with a flexible switching table," *Energies*, vol. 13, no. 8, Apr. 2020, doi: 10.3390/en13081907.

[13]   K. Zhang, M. Fan, Y. Yang, Z. Zhu, C. Garcia, and J. Rodriguez, "Field enhancing model predictive direct torque control of permanent magnet synchronous machine," *IEEE Transactions on Energy Conversion*, vol. 36, no. 4, pp. 2924–2933, Dec. 2021, doi: 10.1109/TEC.2021.3070339.

[14]   M. Schenke and O. Wallscheid, "A deep q-learning direct torque controller for permanent magnet synchronous motors," *IEEE Open Journal of the Industrial Electronics Society*, vol. 2, pp. 388–400, 2021, doi: 10.1109/OJIES.2021.3075521.

[15]   S. A. Q. Mohammed, H. H. Choi, and J.-W. Jung, "Improved iterative learning direct torque control for torque ripple minimization of surface-mounted permanent magnet synchronous motor drives," *IEEE Transactions on Industrial Informatics*, vol. 17, no. 11, pp. 7291–7303, Nov. 2021, doi: 10.1109/TII.2021.3053700.

[16]   M. J. Navardi, J. Milimonfared, and H. A. Talebi, "Torque and flux ripples minimization of permanent magnet synchronous motor by a predictive-based hybrid direct torque control," *IEEE Journal of Emerging and Selected Topics in Power Electronics*, vol. 6, no. 4, pp. 1662–1670, Dec. 2018, doi: 10.1109/JESTPE.2018.2834559.

[17] Z. Zhong, J. You, and S. Zhou, "Torque ripple reduction of DTC based on an analytical model of PMSM," *World Electric Vehicle Journal*, vol. 11, no. 1, Mar. 2020, doi: 10.3390/wevj11010028.

[18] M. Liu *et al.*, "Dual cost function model predictive direct speed control with duty ratio optimization for PMSM drives," *IEEE Access*, vol. 8, pp. 126637–126647, 2020, doi: 10.1109/ACCESS.2020.3007627.

[19] Y.-H. Li *et al.*, "Hybrid decision based on DNN and DTC for model predictive torque control of PMSM," *Symmetry*, vol. 14, no. 4, Mar. 2022, doi: 10.3390/sym14040693.

[20] K. Ullah, J. Guzinski, and A. F. Mirza, "Critical review on robust speed control techniques for permanent magnet synchronous motor (PMSM) speed regulation," *Energies*, vol. 15, no. 3, Feb. 2022, doi: 10.3390/en15031235.

[21] V. Pushparajesh, N. B. M., and H. B. Marulasiddappa, "Hybrid intelligent controller based torque ripple minimization in switched reluctance motor drive," *Bulletin of Electrical Engineering and Informatics (BEEI)*, vol. 10, no. 3, pp. 1193–1203, Jun. 2021, doi: 10.11591/eei.v10i3.3039.

[22] S. G. Petkar and V. K. Thippiripati, "A novel duty-controlled DTC of a surface PMSM drive with reduced torque and flux ripples," *IEEE Transactions on Industrial Electronics*, vol. 70, no. 4, pp. 3373–3383, Apr. 2023, doi: 10.1109/TIE.2022.3181405.

[23] Y. Luo, X. Zhang, and S. Niu, "A hybrid two-stage control solution for six-phase PMSM motor with improved performance," *IEEE Journal of Emerging and Selected Topics in Power Electronics*, vol. 10, no. 5, pp. 5435–5445, Oct. 2022, doi: 10.1109/JESTPE.2022.3141487.

[24] M. Farhat, S. Kamel, A. M. Atallah, and B. Khan, "Optimal power flow solution based on jellyfish search optimization considering uncertainty of renewable energy sources," *IEEE Access*, vol. 9, pp. 100911–100933, 2021, doi: 10.1109/ACCESS.2021.3097006.

[25] A. Benhammou *et al.*, "Exploitation of vehicle's kinetic energy in power management of two-wheel drive electric vehicles based on ANFIS DTC-SVM comparative study," *International Journal of Hydrogen Energy*, vol. 46, no. 54, pp. 27758–27769, Aug. 2021, doi: 10.1016/j.ijhydene.2021.06.023.

BIOGRAPHIES OF AUTHORS

Hallikeri Basappa Marulasiddappa 🆔 📷 SC ↻ is currently a research fellow at JAIN University, Kanakpura, Karnataka, India. He received his B.E. in Electrical and Electronics Engineering in 2005, at Kuvempu university, Davanagere, Karnataka, India. And M-Tech degree in Power Electronics in 2011 from Visweswaraya Technological University, Belagavi, Karnataka, India. He worked as an assistant professor in various top engineering colleges in Karnataka, India. In total, he has 15 years of teaching experience. Area of Interest Power Electronics and Drives, Electric Vehicle and Artificial Intelligence. He guided many undergraduate students in these areas. He has published many papers in international journals and also at international conferences. He even received a best paper award at an international conference. He can be contacted at Marul.bethur@gmail.com.

Viswanathan Pushparajesh 🆔 📷 SC ↻ has been serving as Associate Professor in the Department of Electrical and Electronics Engineering, School of Engineering and Technology JAIN Deemed to be University since 2017. He has completed his PhD from Anna University in Electrical Engineering specializing in Power Electronics and Special Electrical Drives. He has received the International Best Research Award for the year 2018- 2019 instituted by SDF International, London, UK. Adding to his credit he also received national awards like best academic researcher, Outstanding faculty award, Best faculty award and best placement coordinator from various research organizations. He has published many papers in international and national journals with high impact factors. He has received a fund from AICTE worth Rs. 660,000/-for Power Electronics laboratory in MODROB scheme in the Academic Year 2012-2013. He can be contacted at pushparajesh.v@gmail.com.